



Modifying Structural, Optical, and Electrical Features of PVA/CMC/PVP Blend Doped with ZnWO₄ and TPAI

A. M. El-naggar¹ · Zein K. Heiba² · Mohamed Bakr Mohamed^{2,3} · A. M. Kamal¹

Received: 29 January 2024 / Accepted: 4 April 2024

© The Author(s), under exclusive licence to Springer Science+Business Media, LLC, part of Springer Nature 2024

Abstract

Zinc tungstate (ZnWO₄) and tetrapropylammonium iodide (TPAI) are attracted materials that can be applied in different fields such as dye-sensitized solar cells or ultra-high capacitance supercapacitors. Newly blended polymers reinforced using ZnWO₄ nanoparticles and TPAI were fabricated and explored. Poly (vinyl alcohol)/carboxymethyl cellulose/ poly(vinyl pyrrolidone)/ ZnWO₄/x wt % TPAI (PVA/CMC/PVP/ZnWO₄/x wt % TPAI) blended polymers were formed using hydrothermal and solution-casting procedures. X-ray diffraction, transmission electron microscopy, diffused reflectance and fluorescence techniques were used to characterizations the formed blends. The direct and indirect optical band energy values diminished to their minimum values (4.84, 3.97) eV and (4.21, 3.23, 2.96) eV as the blend doped with ZnWO₄ and 0.05 wt% TPAI, respectively. Blend doped with ZnWO₄ and 0.1 wt % TPAI achieved the highest refractive index and optical dielectric constant values. The fluorescence intensities of doped PVA/CMC/PVP blends affected by the kind of dopant and the measuring wavelength range. The addition of ZnWO₄ and/or TPAI samples to the blend enhances their nonlinear optical parameters. According to CIE chromaticity coordinates (x, y) and based on the amount of TPAI doping, doped blends revealed the changeable degrees of blue color. The values of dielectric constant are enhanced slightly as the PVA/CMC/PVP blend loaded with the ZnWO₄ sample and enhanced further as the amount of TPAI doping increased. The σ_{ac} value of the PVA/CMC/PVP blend was improved as the ZnWO₄ sample was added and enhanced further as the content of TPAI doping increased. Loading the PVA/CMC/PVP blend with ZnWO₄ sample reduced its energy density, and raising the TPAI doping amount further reduced it. The formed materials are promising for various applications, such as optoelectronics and energy storage.

Keywords PVA/CMC/PVP, TPAI, ZnWO₄ · Energy storage · Electrical · Optical

1 Introduction

In recent years, polymer blends have emerged as a strategic approach to improving the performance of materials, replacing the use of a single polymer in various device applications [1]. Poly (vinyl alcohol) (PVA) exhibits exceptional properties including superior elasticity, flexibility, non-toxicity, and high thermal stability [2]. Poly(vinyl pyrrolidone) (PVP) is a

distinctively fragile stretching polymer with the capacity to bind polar molecules owing to its polarity [3]. PVP is utilized in various applications as a stabilizing agent in solar cells, a flexible dielectric coating, inks, paints, and food adhesives [4]. Cellulose gum, also known as sodium salt-carboxymethyl cellulose (CMC), is a semicrystalline polysaccharide found in the fibrous tissue of plants. This polymer has the ability to form a gel, interact with other polymers that dissolve in water, and effectively respond to ionic dopants due to the presence of hydroxyl (-OH) and carboxylic anion (COO) groups [5].

In addition, the presence of bulky cations such as TEA⁺ (tetraethylammonium), TBA⁺ (tetrabutylammonium), and TPA⁺ (tetrapropylammonium) in salts like tetraethylammonium iodide (TEAI, C₈H₂₀IN), tetrabutylammonium iodide (TBAI, C₁₆H₃₆IN), and tetrapropylammonium iodide (TPAI, C₁₂H₂₈IN) is responsible for the separation of the polymer matrix. This separation creates more space, allowing smaller

✉ Mohamed Bakr Mohamed
mbm1977@yahoo.com

¹ Physics & Astronomy Department, College of Science, King Saud University, P.O. Box 2455, 11451 Riyadh, Saudi Arabia

² Physics Department, Faculty of Science, Ain Shams University, Cairo, Egypt

³ Physics Department, Faculty of Science, Taibah University, Al-Madina al Munawarah, Saudi Arabia

cations to move more freely [6]. Iodide anions, which have a higher energy, work better with dye-sensitized solar cells (DSSCs) [7].

Zinc tungstate (ZnWO_4) is classified as a binary metal oxide belonging to the AWO_4 group of metal oxides [8]. As a class of inorganic materials, metal tungstate shows great promise in a number of areas because of its high oxidation states and similarities to hybrid oxides [9]. Along with being an inexpensive and eco-friendly element, zinc has shown promising electrical and electrochemical activity when mixed with other elements [10]. This means that ZnWO_4 , a compound containing both zinc and metal tungstate, has a wide range of potential physical and chemical uses, such as gas sensors, electrochemical devices, and ultra-high capacitance supercapacitors [11, 12].

Moreover, the characteristics of polymers make them suitable for serving as hosts for a wide range of fillers. Polymer composites have the potential to fulfil various uses in optoelectronics, shielding, optical devices, photocatalysts, sensors, solar cells, supercapacitors, and medicine [13]. The properties of a polymer or blended polymer can be modified as it is doped with a suitable element or irradiated with suitable source. For instance, the addition of (SiC-BaTiO_3) nanoparticles to PVA resulted in improved optical, structural, and A.C electrical characteristics. This enhancement makes the (PVA-SiC-BaTiO₃) nanostructures highly potential materials for a wide range of optoelectronic nanodevices [14]. PVC films that have been altered by light exposure are appropriate as anti-reflected coatings and work well in high refractive lenses and photovoltaic cell usage [15]. Al-Azzawi et al. found that PVA/silicon carbide thin films have a wide range of optoelectronic applications, including solar cells and inexpensive electronic devices for spectroscopic characteristics and electronics [16]. CuO and CoO-doped poly(vinyl chloride) thin films have a high solar energy absorption capacity [17]. The nonlinear optical parameters exhibited a rise as the concentration of FeCl_3 in the PVA matrix rose. The PVA/ FeCl_3 composite polymer films demonstrated potential for use in flexible optoelectronic applications [18]. Alawi et al. synthesized a novel ternary blend polymer consisting of poly(acrylamide), poly(vinyl alcohol)/poly(vinyl pyrrolidone)/ SiO_2 for use in solar cells, optoelectronic devices, and biology applications [19]. The amount of ($\text{SrTiO}_3\text{-CoO}$) nanoparticles in PEO/PVA blend directly correlates with a rise in the refractive index, extinction coefficient, dielectric constant, and optical conductivity of the host matrix. This characteristic makes it a promising candidate for photonics applications [20]. The nanocomposite films composed of PVA/ $\text{SiO}_2\text{-CuO}$ demonstrate substantial attenuation coefficients upon exposure to gamma rays [21]. The nanocomposites consisting of PVA-PVP-ZrC have been identified as highly promising for flexible optoelectronic applications [22]. Adding carbon quantum dots

to PVA/ Bi_2O_3 polymer nanocomposite films significantly increased their yellowness [23]. Polyethylene oxide and carboxymethylcellulose doped with CuCo_2O_4 were found by Ragab et al. to have potential optoelectronic applications [24]. $\text{Ni}_{0.65}\text{Cu}_{0.35}\text{Fe}_2\text{O}_4$ additives can be used to customize PVA/CMC blend films, making them suitable for use in optical devices [25]. Blends of poly (methyl methacrylate) (PMMA), polyethylene oxide (PEO), vanadium-doped nano titanium dioxide (TiO_2/V), and tetrabutylammonium iodide (TBAI) may be used as optical materials in the development of upcoming flexible optoelectronic devices. After being doped with TiO_2/V and TBAI, PMMA/PEO's UV absorbance significantly increased, suggesting that the doped blend could be used as UV blocking in greenhouse settings [26]. Films made of poly (vinyl chloride) (PVC), polyethylene glycol (PEG), nano cerium dioxide, and TBAI exhibit promise as energy storage devices and good absorbers of various UV spectra [27]. In comparison to the undoped blend, the PVP/CMC blend with hydrogen titanate nanotubes (HTNT) and 0.1 wt % TMAI has the highest energy density [3]. A variety of optoelectronic applications, including sensors and polymer-based capacitors in energy storage devices, have been suggested for PVC/ FeCr_2O_4 / tetrapropylammonium iodide (TPAI) due to their improved dielectric characteristics [28].

By incorporating ZnWO_4 and varying concentrations of TPAI, this study aims to enhance the optical and dielectric properties of the PVA/CMC/PVP blend, which could find applications in optoelectronics and energy storage systems. Therefore, PVA/CMC/PVP/ ZnWO_4/x wt % TPAI blended polymer were formed using hydrothermal and solution-casting procedures. All properties were investigated using different techniques such as XRD, TEM, diffused reflectance, FL spectroscopy, LCR meter. In addition, using suitable analytical methods, this research thoroughly examines the electrical, optical, and energy density properties of these formed blends.

2 Methods and Materials

2.1 Preparation of ZnWO_4 Sample

In order to produce ZnWO_4 , sodium tungstate dihydrate (Sigma-Aldrich, 99%) and zinc nitrate hexahydrate (Sigma-Aldrich, 98%) were dissolved in 90 ml of deionized water and stirred magnetically for 1 h. A Teflon-lined stainless steel autoclave was used to heat the resultant solution to 180 °C for 20 h. After that, the autoclave was left to cool down to room temperature (*RT*). A final product was obtained through a series of centrifugal and washing steps using ethanol and deionized water. The powder was

prepared, dried, and then annealed in an electric oven for 1 day at 60 °C.

2.2 Preparation of PVA/CMC/PVP/ZnWO₄/x wt% TPAI Blended Polymer

The casting procedure was employed to produce PVA/CMC/PVP (0.7:0.2:0.1) blend, 0.7 g of polyvinyl alcohol (PVA, MW = 50,000 g/mol, Sigma Aldrich), 0.2 g carboxymethyl cellulose (CMC, in the form of the sodium salt of commercial grade, Sigma Aldrich) and 0.1 g polyvinyl pyrrolidone (PVP, MW = 40,000 g/mol, Sigma Aldrich) were dissolved in 70, 20 and 10 ml deionized at 70 °C, 50 °C and *RT*, respectively. After letting each solution cool to *RT*, they were mixed for 2 h at *RT*. The resulting solution was transferred into a Petri dish and subsequently subjected to 40 °C in an oven for 4 days. The previous step was repeated with 3 wt % ZnWO₄ and different concentrations of tetrapropylammonium iodide (TPAI, Sigma Aldrich, 98%) in order to create PVA/CMC/PVP/ZnWO₄/x wt% TPAI blends (*x* = 0, 0.05, 0.1, 0.15, and 0.2 wt%). The thickness of the generated blends ranges from

220 to 340 μm, as measured using a digital micrometer with a precision of ± 10 μm.

2.3 Characterization Techniques

The ZnWO₄ and all blend structures were investigated using a PANalytical X-ray diffractometer (X'pert MPD model, copper source). The transmission electron microscope (TEM, JEM-2100 electron microscope, JEOL Ltd, Japan, 200 kV) was used to examine the fillers' crystallite size. To create the fluorescence (*FL*) spectra, the FP-8200 JASCO luminescence spectrophotometer was used.

The UV diffuse reflectance (*R*) and transmittance (*T*) data for all blends were gathered utilizing a JASCO-V-670 diffuse reflectance spectrophotometer that was associated with an integrating sphere assembly. The following steps are taken to correct the *R* value:

$$R_i = \frac{[2 + T^2 - (1 - R)^2] - \left\{ [2 + T^2 - (1 - R)^2]^2 - 4(2 - R)R \right\}^{0.5}}{2(2 - R)} \quad (1)$$

$$R_F = (2 + T^2 - (1 - R_i)^2 - \left\{ [2 + T^2 - (1 - R_i)^2]^2 - 4R_i(2 - R_i) \right\}^{0.5}) (2(2 - R_i))^{-1} \quad (2)$$

Where *R_i* and *R_F* are the interface reflectance and reflection from one face, respectively.

The absorbance (*A*), coefficients of extinction (*k*), and refractive index (*n*) for each blend were determined via the subsequent formulas:

$$A = \ln\left(\frac{R_F T}{R_i - R_F}\right) \quad (3)$$

$$k(R_i, T) = \frac{\lambda}{4\pi d} \ln\left[\frac{R_F(R_i, T)T}{R_i - R_F(R_i, T)}\right] \quad (4)$$

$$n = \frac{1 + R_F(R_i, T)}{1 - R_F(R_i, T)} + \left\{ \frac{4R_F(R_i, T)}{(1 - R_F(R_i, T))^2} - \left(\frac{\lambda}{4\pi d}\right)^2 \ln^2\left[\frac{R_F(R_i, T)T}{R_i - R_F(R_i, T)}\right] \right\}^{0.5} \quad (5)$$

The real (ϵ_r) and imaginary (ϵ_i) components of the dielectric constant, the surface energy loss function (SELF) volume energy loss function (VELF), optical conductivity (σ_{opt}), linear optical susceptibility ($\chi^{(1)}$), nonlinear optical susceptibility ($\chi^{(3)}$), and nonlinear refractive index (n_2) parameters for the different blends were gotten by means of the succeeding equations [1–3]:

$$\epsilon_r = n^2 - k^2 \quad (6)$$

$$\epsilon_i = 2nk \quad (7)$$

$$SELF = \frac{\epsilon_i}{(\epsilon_r + 1)^2 + \epsilon_i^2} \quad (8)$$

$$VELF = \frac{\epsilon_i}{\epsilon_r^2 + \epsilon_i^2} \quad (9)$$

$$\sigma_{opt} = \frac{\alpha n C}{4\pi} \quad (10)$$

$$\chi^{(1)} = \frac{1}{4\pi} (n^2 - 1) \quad (11)$$

$$\chi^{(3)} = 1.7 * 10^{-10} (\chi^{(1)})^4 = 1.7 * 10^{-10} \left(\frac{n^2 - 1}{4\pi}\right)^4 \quad (12)$$

$$n_2 = \frac{12\pi}{n} \chi^{(3)} \quad (13)$$

where c is velocity of the light.

Using a GwINSTEK LCR 8105G instrument with a 2 V ac voltage, one can determine the dielectric constant parameters at RT as a function of frequency by measuring the changes in capacitance (C) and dissipation factor ($\tan \delta$).

Each blend's dielectric constant (ϵ' , ϵ''), ac conductivity (σ_{ac}), and complex electric modulus ($M^* = M' + iM''$) were calculated using the following equations [1–3]:

$$\epsilon' = Cd/\epsilon_0A \quad (14)$$

$$\sigma_{ac} = 2\pi f \epsilon_0 \epsilon' \tan \delta \quad (15)$$

$$\tan \delta = \epsilon''/\epsilon' \quad (16)$$

$$M' = \frac{\epsilon'}{\epsilon'^2 + \epsilon''^2} \quad (17)$$

$$M'' = \frac{\epsilon''}{\epsilon'^2 + \epsilon''^2} \quad (18)$$

where ϵ_0 and A are the permittivity of free space and area of the disc, respectively.

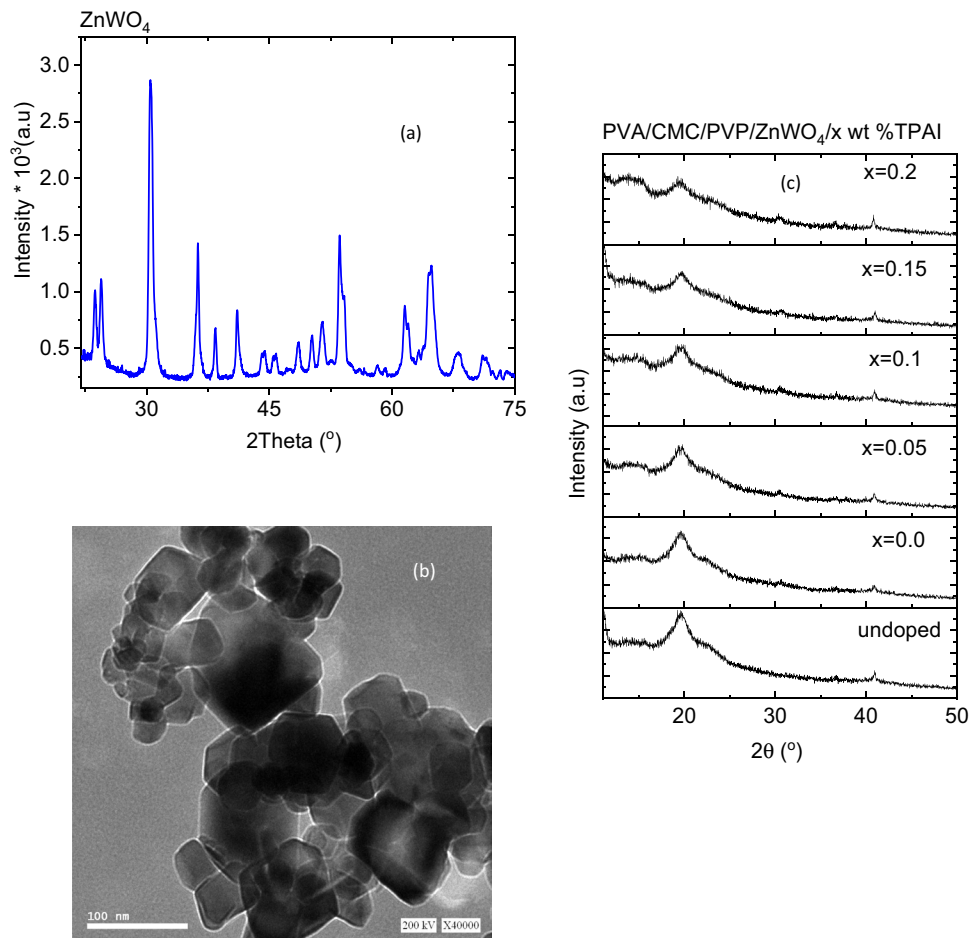
3 Results and Discussion

3.1 Structural Investigation

3.1.1 Structure and Microstructure of $ZnWO_4$

The X-ray diffraction (XRD) data for $ZnWO_4$ filler are displayed in Fig. 1a. The plot shows that the $ZnWO_4$ sample has a monoclinic structure (P2/c) with diffraction peaks at $2\theta = 23.68^\circ, 24.53^\circ, 30.52^\circ, 36.35^\circ, 38.43^\circ, 41.11^\circ, 44.34^\circ, 45.87^\circ, 48.55^\circ, 50.24^\circ, 51.47^\circ, 53.78^\circ, 61.53^\circ, 64.83^\circ, 68.14^\circ$ and 71.44° . These diffraction peaks relate to (011), (110), (-111)/(111), (021)/(002), (200), (121), (112), (211), (220), (130), (-202), (202), (113), (-311), (121) and (041) crystallographic planes, respectively [29]. The following Scherrer formula indicates that the sample's average crystallite size is 45 nm:

Fig. 1 a XRD pattern and b TEM image for $ZnWO_4$ and c XRD patterns for PVA/CMC/PVP/ $ZnWO_4$ /x wt % TPAI blends



$$D = \frac{0.9\lambda}{\beta \cos\theta} \quad (19)$$

where λ and β are the wavelength of the X-ray technique and the full width at half maximum intensity, respectively.

The ZnWO_4 filler sample had an average particle size of 50 nm, based on a transmission electron microscopy image, Fig. 1b.

3.1.2 Structure of PVA/CMC/PVP/ ZnWO_4/x wt % TPAI Blends

Figure 1c shows the XRD patterns of the PVA/CMC/PVP/ ZnWO_4/x wt % TPAI blends. The graph, displays high diffuse scattering, owing to the amorphous nature of the polymer blends, superimposed with a main broad peak around $2\theta = 19.6^\circ$ and a weak peak around $2\theta = 40.9^\circ$. The peak around $2\theta = 21^\circ$ belongs to the characteristic peaks of PVA and PVP [30, 31], and the small peak at $2\theta \sim 41^\circ$ is associated with the overlapped peaks of PVA [32]. The diffraction data between the undoped and doped PVA/CMC/PVP blends do not show any significant differences, indicating that the filler is distributed uniformly throughout the blend matrix.

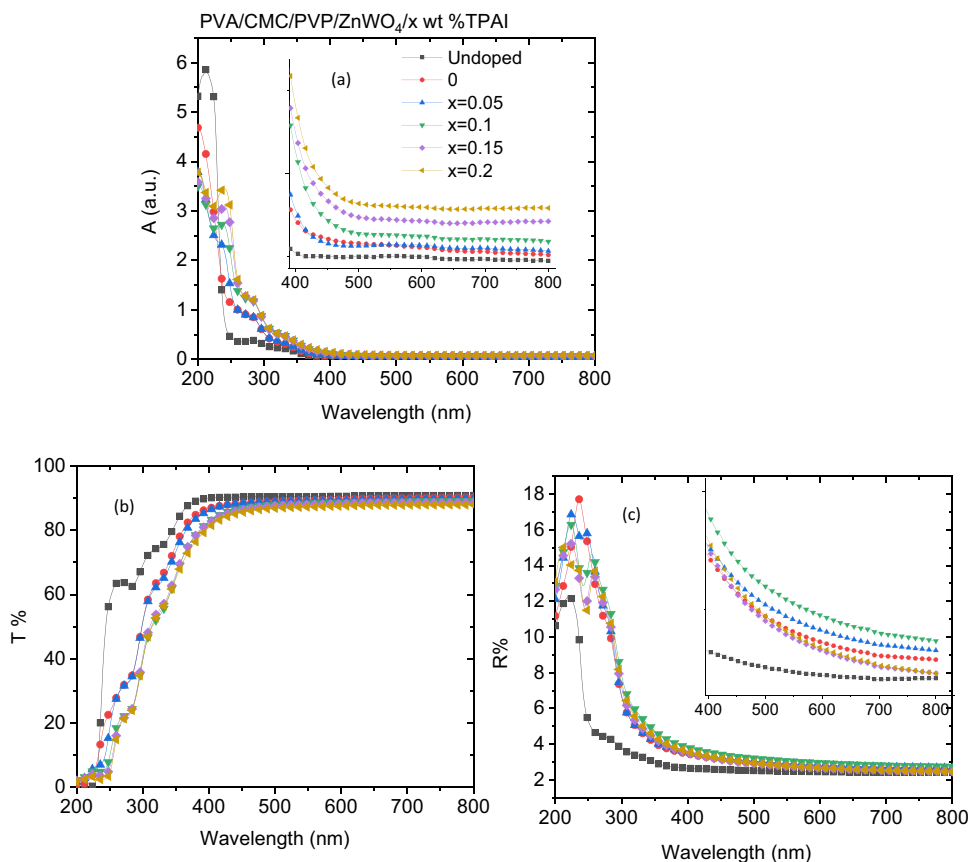
3.2 Optical Features

3.2.1 Absorption, Transmission and Reflectance Spectra of the Blends

In order to study the induced changes to the intermolecular structure of polymeric substances, it is essential to analyze the absorption, transmission and reflectance spectra. This might be a crucial element in clarifying the interior composition of the energy gap. The absorption spectra of PVA/CMC/PVP/ ZnWO_4/x wt % TPAI blends are shown in Fig. 2a. The graph established a similar attitude a sharp inclination with increasing wavelength (λ) followed by a slow one at higher values of wavelength. The excellent miscibility of these blends and fillers is demonstrated by these changes. The absorption peak is situated at ~ 212 nm owing to the $n-\pi^*$ transition, which is produced from unsaturated C–O and/or C–C bonds found in the tail–head of PVA [33]. The ZnWO_4 filler is associated with the second band that emerged at 240 nm [34, 35]. Furthermore, as the PVA/CMC/PVP blend was doped with ZnWO_4 or TPAI, its absorption decreased up to $\lambda = 230$ nm.

Above this range, the blend's absorption goes up a little more when it is loaded with ZnWO_4 , and it goes up even

Fig. 2 a Absorption, b transmittance and c reflectance spectra as a function of the incident wavelength for PVA/CMC/PVP/ ZnWO_4/x wt % TPAI blends



more when more TPAI is added. As the blend is doped with ZnWO_4 and/or TPAI fillers, induced variations in the energy gap region are demonstrated by a red shift in the absorbance spectra. The rise in absorption values observed with ZnWO_4 and TPAI can be attributed to a reduction in the quantity of hydrogen bonds that existed within the polymers during the doping procedure. Nanocomposite polymers are becoming more amorphous, according to the findings [36]. Our findings are similar to those of other researchers, including PVA PVP/PEG polymeric sheets doped with NiO or ZnO/Co doped PVA polymer [37]. According to our results, the optical properties of the PVA/CMC/PVP blend are most controlled by the TPAI concentration. Each blend's transmission spectra are displayed in Fig. 2b. It appears that the decrease in transmission is in line with the rise in absorption that has been noted. Transmission data in the ultraviolet (UV) range is significantly lower for PVA/CMC/PVP blends loaded with ZnWO_4 and TPAI samples compared to undoped samples, while transmission data in the visible range reveals a small reduction with increasing TPAI concentration. Similar results were noticed as PVA/PVP polymeric blend doped with potassium dichromate [38]. This shows that the filler composition has a significant impact on the scattering process through the blends that were studied. This process is generally considered the main factor that impacts transmission through the different

samples [39]. It also provides a detailed description of the common interactions between the samples' medium and the incident light photons, as well as the variations within the host blend matrix. Also, as the PVA/CMC/PVP blend was doped with ZnWO_4 and TPAI amounts, the R values rose irregularly. The high R value was observed in the blend with 0.1wt% TPAI and ZnWO_4 . Adding ZnWO_4 and TPAI to the host blend changes its packing density, and hence its reflectance [40].

3.2.2 Optical Band Gaps of the Blends

To investigate the changes in the internal structure of the band gap region, one can use the following relation [1–3]:

$$(\alpha h\nu) = H(h\nu - E_g)^m \quad (20)$$

where E_g are band gap values for both types of blends (doped and undoped), H and $h\nu$ represent the energy independent parameter and the incident photon energy, respectively. The value of the parameter m specifies the nature of the transition; $m = \frac{1}{2}$ for direct allowed transitions and $m = 2$ for indirect allowed transitions.

Figure 3 illustrates the direct and indirect E_g values of all blends. The values of E_g are determined by extrapolating the linear segment of the graphs at the zero points of $(\alpha h\nu)^2$

Fig. 3 a, b Direct and c, d indirect Tauc's relations for PVA/CMC/PVP/ ZnWO_4/x wt % TPAI blends

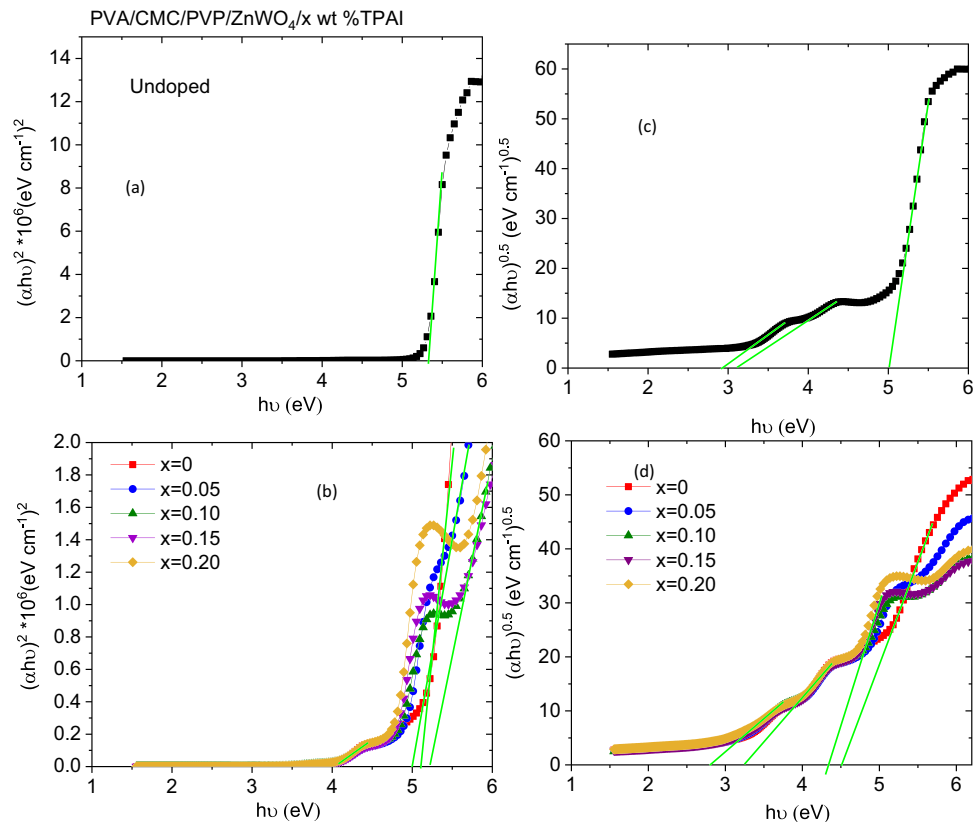


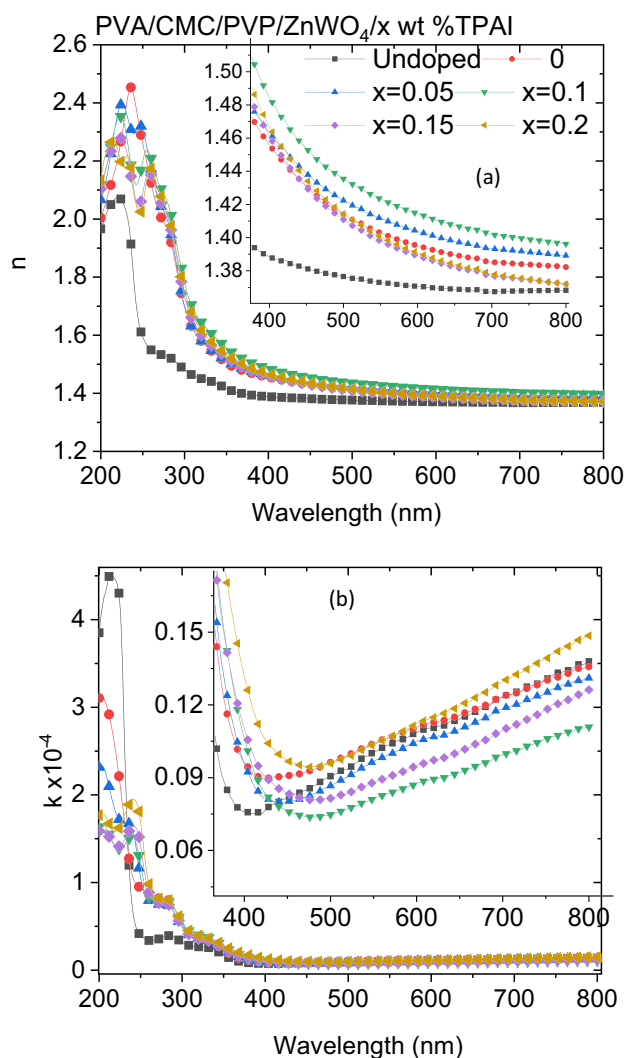
Table 1 Direct and indirect optical band gap energies and chromaticity coordinates (x, y) for the normalized FL spectra represented under 434 nm excitation wavelength of PVA/CMC/PVP/ZnWO₄/x wt % TPAI blends

Sample	Direct E_g (eV)	Indirect E_g (eV)	CIE coordinates
PVA/CMC/PVP	5.32	5.01, 3.26, 2.98	(0.2164, 0.2985)
PVA/CMC/PVP/ZnWO ₄ /x wt % TPAI			
x=0	5.11, 4.99, 3.97	4.52, 3.23, 2.96	(0.1909, 0.2667)
x=0.05	4.84, 3.97	4.21, 3.23, 2.96	(0.2177, 0.2947)
x=0.1	5.22, 4.83, 3.97	4.05, 3.23, 2.96	(0.2164, 0.2985)
x=0.15	5.22, 4.78, 3.96	4.34, 3.24, 2.97	(0.2228, 0.2943)
x=0.2	5.3, 4.76, 3.97	4.29, 3.23, 2.82	(0.2389, 0.2853)

and $(\alpha h\nu)^{0.5}$. The direct and indirect E_g values diminished from 5.32 eV and (5.01, 3.26, 2.98) eV (for PVA/CMC/PVP blend) to (5.11, 4.99, 3.97) eV and (4.52, 3.23, 2.96) eV (for doped PVA/CMC/PVP with ZnWO₄), and decreased irregularly more as it doped with TPAI, reaching their minimum values (4.84, 3.97) eV and (4.21, 3.23, 2.96) eV as the blend doped with 0.05 wt % TPAI, respectively, as listed in Table 1. A rise in disorder of the host blend structure as a result of doping causes an increase in localized states inside the band gap region, which in turn causes this decrease. A rise in the number of disorders occurred because fillers reduced the number of hydrogen bonds inside the host blend chain. This is evidence of the fillers' strong bond to the blend base. Lithium titanate nanoparticles have been demonstrated in the literature to lower the E_g values of carboxymethyl cellulose/polyacrylamide blend, which is consistent with our findings [41].

3.2.3 Refractive Index and Extinction Coefficient of the Blends

The refractive index (n) is a fascinating optical parameter because of its promising characteristics, especially for optical materials. It is extensively utilized in the industry to control the operations of various communication and optoelectronic devices, including modulators, electronic detectors, filters and displays. It is largely dependent on the degree of polarization of the medium's molecules. Moreover, the extinction coefficient (k) is a property inherent to the material that determines how well incident light of a particular wavelength can be absorbed or reflected. For every blend, the relationship between the incident photon wavelength and (n and k) is displayed in Fig. 4. The graph revealed that all blends' n values exhibited normal dispersion. Compared to the undoped blend, the doped blend has a higher n value. The blend that was doped with ZnWO₄ and 0.1 wt % TPAI achieved the highest n value. Composite polymers made of silicon-doped polyvinyl

**Fig. 4** **a** Refractive index and **b** extinction index for PVA/CMC/PVP/ZnWO₄/x wt % TPAI blends

alcohol (PVAOH) also showed similar results [42]. Since n is a density-sensitive parameter, a higher value for n suggests that the blend matrix and fillers are forming more bonds, which lowers the likelihood of hydrogen bond formation but rises the number of disorders and, in the end, the density of the compound. Hence, the optical density and structure of the PVA/CMC/PVP blend were altered by incorporating ZnWO₄ and TPAI. This led to changes in the doped blend's n values [43]. Furthermore, the k values were altered upon loading the PVA/CMC/PVP blend with ZnWO₄ and TPAI. The number of hydrogen bonds within the polymer was reduced during the doping and miscibility processes, which caused the k values to rise. Additionally, the doped blend's filler samples may absorb

or scatter some of the photon's energy, which could alter k 's value [44].

3.2.4 Optical Dielectric Constant of the Blends

Figure 5 illustrates the relationship between wavelength and the real and imaginary dielectric constants (ϵ_r , ϵ_i) of PVA/CMC/PVP/ZnWO₄/x wt % TPAI blends. It also shows the spectra of the surface and volume energy loss functions (SELF and VELF). The graphs indicated that ϵ_r and ϵ_i displayed similar characteristics, n and k , respectively. Both ϵ_r and ϵ_i attain their highest values in the UV region. Throughout the entire wavelength range, doped blends exhibited an increase in both ϵ_r and ϵ_i . Additionally, VELF values exceed SELF values for each blend. The SELF and VELF curves both had patterns that were comparable to the ϵ_i curve. The introduction of ZnWO₄ and TPAI fillers resulted in a modification of the density of the localized state levels that are formed between the highest occupied molecular orbital (HOMO) and the least unoccupied molecular orbital (LUMO). This modification subsequently impacts the ϵ_r value of the PVA/CMC/PVP blend. The fluctuating ϵ_i value [45, 46] is attributed to variations in the dipole motion. Figure 6 displays the relationship between the optical conductivity (σ_{opt}) and the wavelength of incident light for PVA/CMC/PVP/ZnWO₄/x wt % TPAI blends. The plot

Fig. 5 a ϵ_r , b ϵ_i , c SELF and d VELF spectra for PVA/CMC/PVP/ZnWO₄/x wt % TPAI blends

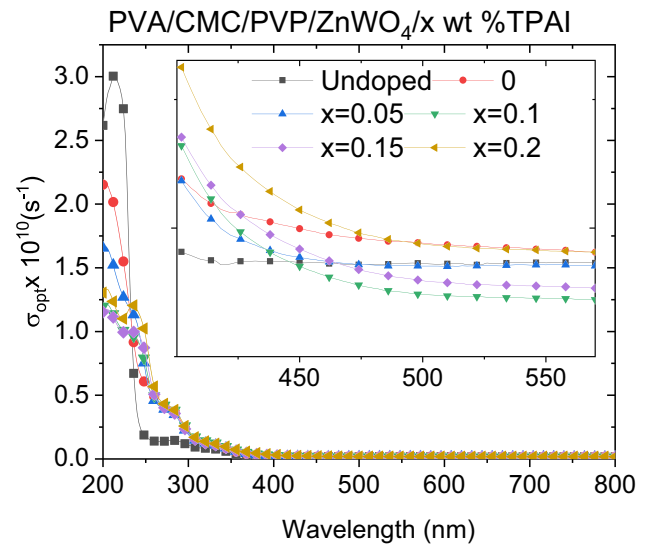
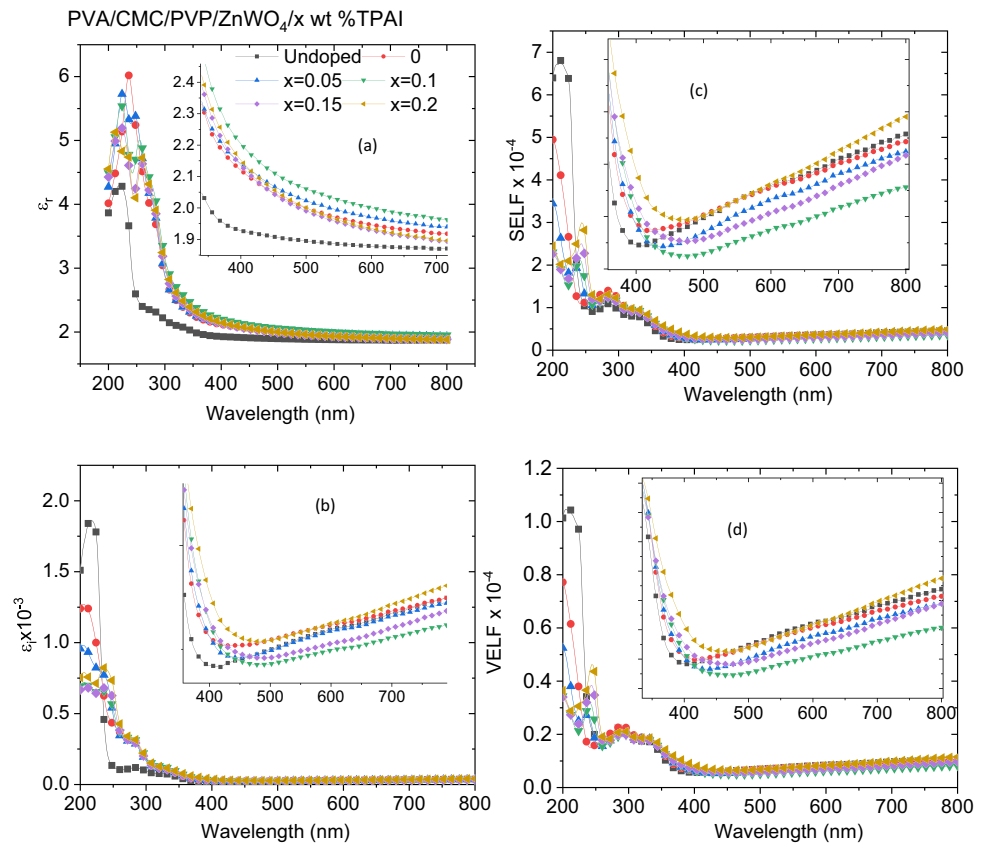


Fig. 6 Wavelength dependent of the optical conductivity for PVA/CMC/PVP/ZnWO₄/x wt % TPAI blends

showed that adding ZnWO₄ and TPAI samples to the blend enhanced the σ_{opt} value of PVA/CMC/PVP in the UV range. The σ_{opt} value in the visible range changed as a function of the concentration of TPAI doping. The blend doped with ZnWO₄ and 0.2 wt% TPAI showed the greatest σ_{opt} value.

The density of localized states is altered during the doping process, and this could be linked to the appearance of new empty energy levels in the blend structure between the HOMO and LUMO inside the forbidden optical band gap [47].

3.2.5 Nonlinear Optical Parameters of the Blends

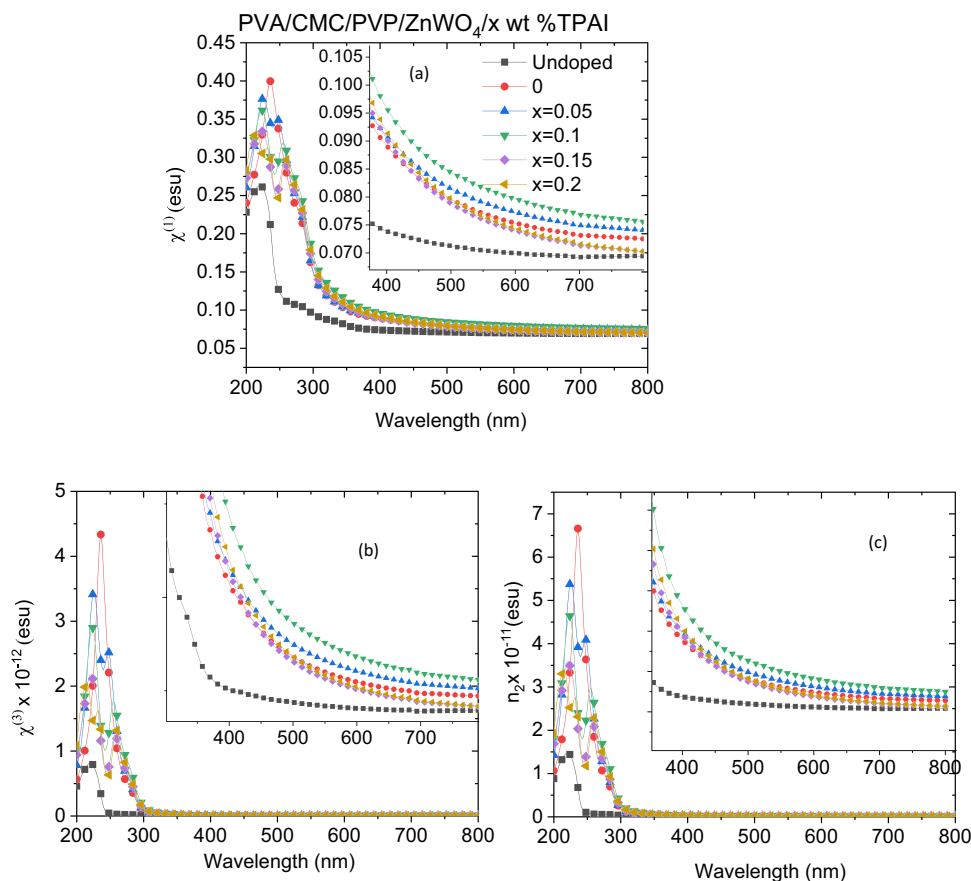
It is possible to assess the potential of nanocomposite films for nonlinear optical (NLO) applications by finding their linear optical susceptibility ($\chi^{(1)}$), nonlinear optical susceptibility ($\chi^{(3)}$), and nonlinear refractive index (n_2) parameters. Figure 7 shows the changes in the NLO parameters as a function of wavelength. The graph showed a consistent trend of increasing values for $\chi^{(1)}$, $\chi^{(3)}$, and n_2 as the blend loaded with TPAI and ZnWO₄. The PVA/CMC/PVP blend with 0.1 wt% TPAI and ZnWO₄ has the highest NLO values. A change in the total number of hydrogen bonds during miscibility and doping can account for an increase in NLO parameters values based on the induced modifications in the blend matrix. Because of this, the number of defects or disorders increases, which in turn increases the number of chemical free radicals and their mobility, leading to higher

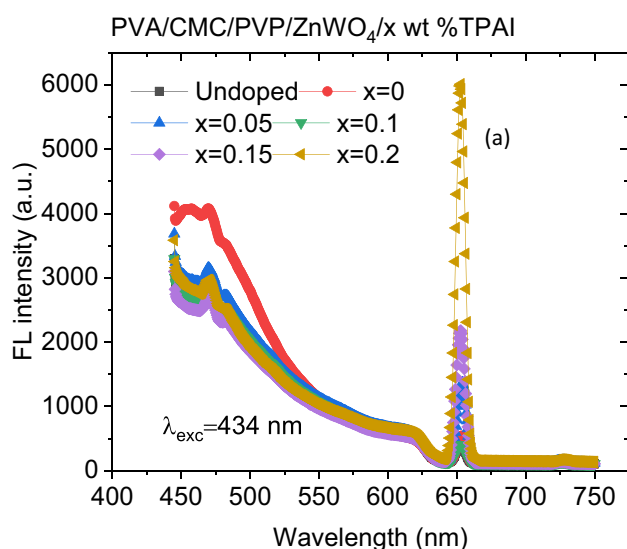
values for NLO parameters [48]. The addition of ZnWO₄ and TPAI samples to our blends enhances their nonlinear optical parameters, making them a potential candidate for future optoelectronic applications.

3.3 Fluorescence Analysis

The fluorescence (FL) spectra of PVA/CMC/PVP/ZnWO₄/x wt % TPAI blends were obtained using 434 nm UV light as the excitation wavelength, Fig. 8a. The graph demonstrates that the FL intensities of the sub-peaks at 450–550 nm in the doped PVA/CMC/PVP blend samples rose when loaded with ZnWO₄, but they decreased when the blend loaded with TPAI in addition. On the contrary, the peak at 650 nm increased as the quantity of TPAI doping increased. Variations in the number of non-radiative defects on the materials' surface and changes in the recombination rate of photo-induced electron (e⁻) and hole (h⁺) pairs within the materials could be the cause of the increasing and decreasing FL intensity [49]. The sub-peaks of the FL spectra can be identified as blue, green, and red colors. Elashmawi et al. observed that the PVP/PVA blend produced both blue and red colors [50]. The blue color correlated with defect-related luminescence. The green emission may be a consequence of

Fig. 7 The nonlinear optical parameters: **a** $\chi^{(1)}$, **b** $\chi^{(3)}$ and **c** n_2 for PVA/CMC/PVP/ZnWO₄/x wt % TPAI blends





CIE chromaticity diagram 1931

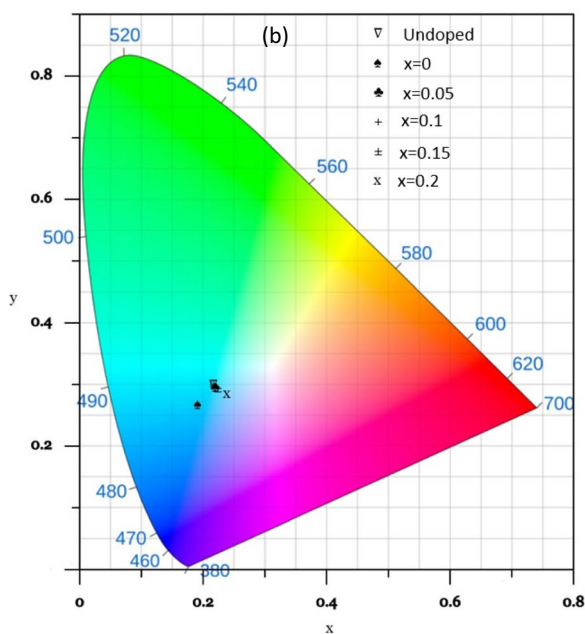


Fig. 8 **a** The FL spectra, and **b** CIE diagrams for PVA/CMC/PVP/ZnWO₄/x wt % TPAI blends

the dopant or impurity atoms. The red emission is a result of the defect-containing materials [51]. Using the 1931 standard (CIE) color space chromaticity diagram of the normalized FL data (Fig. 8a), the calculated colors of the different blends are represented in Fig. 8b. Table 1 reveals the CIE chromaticity coordinates (x , y) for each blend. Based on the amount of TPAI doping, doped blends revealed changeable degrees of blue color.

3.4 Dielectric Characteristics

The suitability of PVA/CMC/PVP/ZnWO₄/x wt% TPAI blends for use in the design of blended polymer-based capacitors was evaluated by analyzing their dielectric characteristics. The dielectric features of different samples can be estimated by finding out the values of the dielectric constant (ϵ') and the dielectric loss (ϵ''). Energy dissipation is measured by the dielectric loss, whereas energy storage capacity is quantified by dielectric constant [52]. Figure 9a and b illustrate the frequency dependence of ϵ' and ϵ'' for all blends. The interfacial polarization causes ϵ' values to be relatively high at low frequencies. At high frequencies, dipoles lose their ability to align with the electric field, resulting in a reduction in the dielectric constant to its minimum value. For each blend, the value of ϵ'' initially decreased, then increased as the frequency increased, reaching a maximum value, and then decreased again. This peak experienced a slight displacement when doped with ZnWO₄ and TPAI. The shift occurs due to the different relaxation times [53]. Furthermore, the values of ϵ' and ϵ'' were enhanced slightly as PVA/CMC/PVP loaded with ZnWO₄ sample and enhanced further as the amount of TPAI doping increased. Both ϵ' and ϵ'' attained their highest values in the blend with $x=0.2$. Similar results were observed as PVA–PVP blend filled with different Ni–Cd concentrations and poly (vinyl chloride-co-vinyl acetate-co-2-hydroxypropyl acrylate) filled with graphene oxide [54, 55]. The value of ϵ' can be altered by a modification in interfacial polarization resulting from a variation in the arrangement of different filler samples within the PVA/CMC/PVP host blend [56].

Electrical conductivity measurements are essential for studying the transport mechanisms in different blends. Figure 9c displays the frequency dependence of the AC conductivity (σ_{ac}) for all blends. As the frequency range increases, all blends exhibit a sharp increase in σ_{ac} values, which remain constant up to 10⁴ Hz. The rise in σ_{ac} can be attributed to the increased frequency of electron hopping at relatively high frequencies. Besides, the σ_{ac} value of PVA/CMC/PVP blend was improved as the ZnWO₄ sample was added and enhanced further as the content of TPAI doping increased. Fillers in a blend matrix have the potential to change the AC conductivity by changing the amount of charge carriers and defects in the polymer [57].

To find the energy density (U) of a blend, one can use the subsequent relation [1–3]:

$$U = \frac{1}{2} \epsilon_0 \epsilon' E^2 \quad (21)$$

where ϵ_0 and E are the permittivity of free space (8.85×10^{-12} F/m) and the electric field, respectively.

Fig. 9 Variation of **a** real and **b** imaginary parts of the dielectric constant with frequency and **c** AC electrical conductivity for PVA/CMC/PVP/ZnWO₄/x wt % TPAI blends

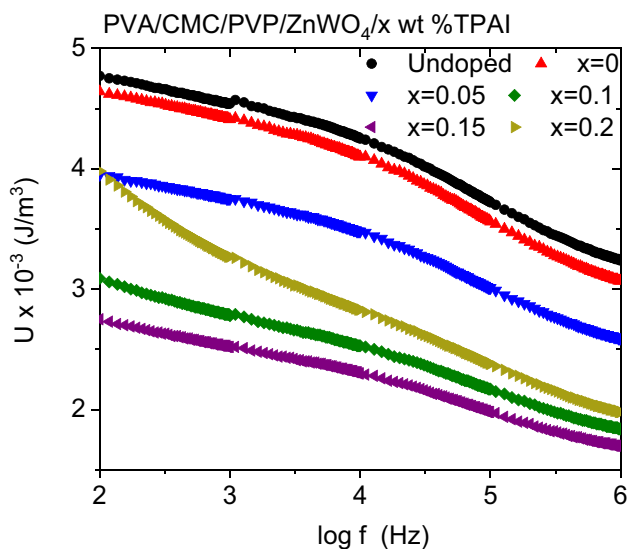
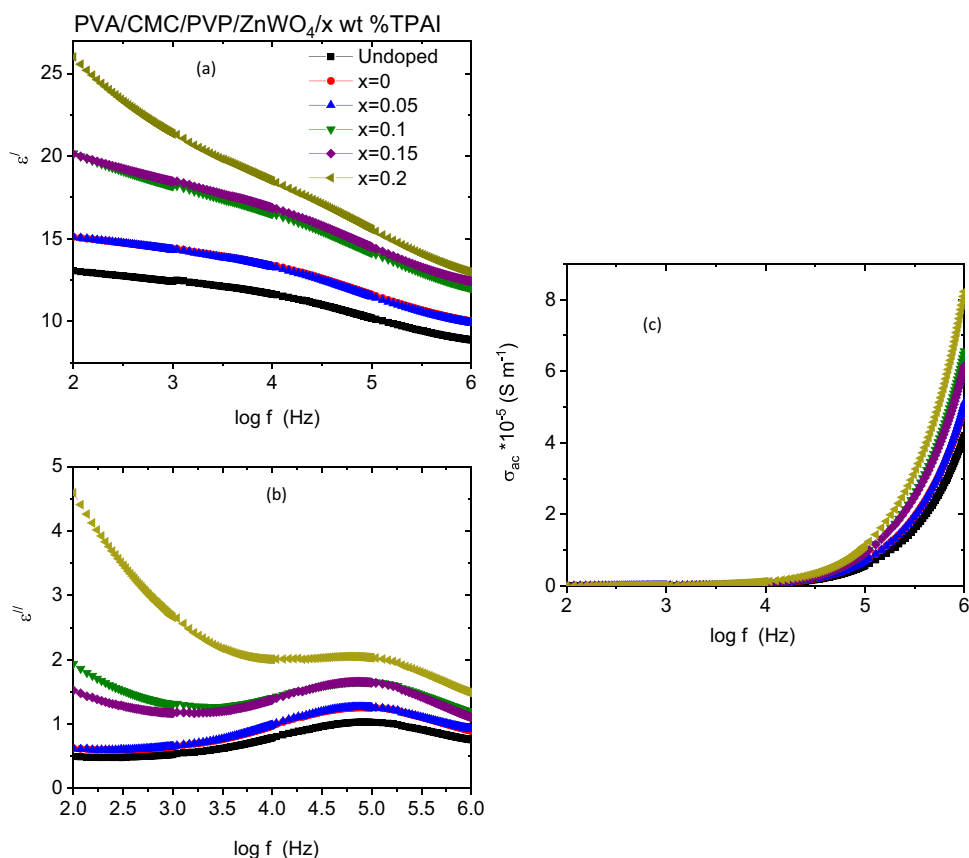


Fig. 10 Variation of energy density for PVA/CMC/PVP/ZnWO₄/x wt % TPAI blends

As seen in Fig. 10, the frequency dependence of U is displayed for all blends. Loading PVA/CMC/PVP blend with ZnWO₄ sample reduced its energy density, and raising the TPAI doping amount further reduced it.

To study the phenomenon of conductivity relaxation and electrode influence, the complex quantity known as the electric modulus (M^*) was examined [58]. The real and imaginary parts of the electric modulus (M' , M'') are plotted as a function of frequency for all blends in Fig. 11. The graph shows that the lowest value of M' happens at low frequencies. These results indicated that the effects of electrode polarization were minor [59]. The M' values of the PVA/CMC/PVP blend were reduced when ZnWO₄ and TPAI samples were loaded into it. Higher frequency unsaturation in M' values was found to be connected with more effective interfacial polarization [60]. Furthermore, all blends showed a peak (one relaxation time) in M'' . Additionally, the M'' modulus curves' relaxation peak is divided into two sections. The first portion is located at low frequency, to the left of the relaxation peak, and it represents the frequency range where ions can travel great distances and quickly transition between nearby sites. The second region, where ions are trapped in their potential wells and can only move locally, is on the right side of the relaxation peak (at high frequency). The relaxation peaks exhibit asymmetry peak broadening, which suggests distinct time constants [61]. Because the host blend has different filler compositions, the intensity and location of this peak changed slightly. As the filler was added, PVA/

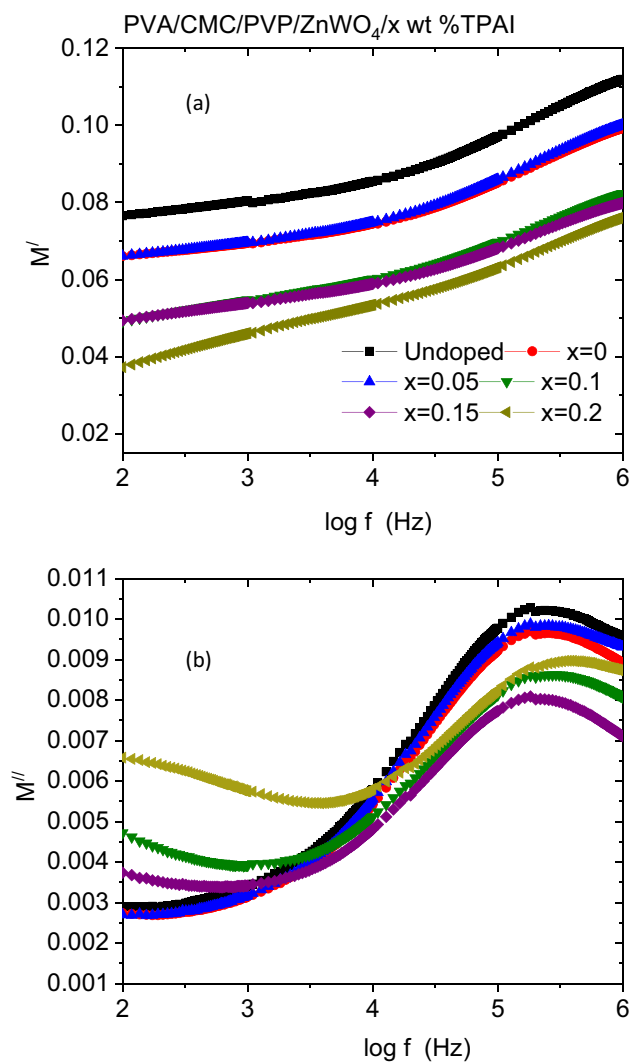


Fig. 11 Frequency dependence of the **a** real and **b** imaginary parts of electric modulus for PVA/CMC/PVP/ZnWO₄/x wt % TPAI blends

CMC/PVP's peak intensity varied, which altered the sample capacitance [58].

4 Conclusions

ZnWO₄ filler has a monoclinic structure (P2/c) with an average particle size of 50 nm. PVA/CMC/PVP/ZnWO₄/x wt % TPAI blends have an amorphous nature. The optical properties of the PVA/CMC/PVP blend are controlled by ZnWO₄ doping and/or TPAI concentration. Transmission data in the UV range is significantly lower for PVA/CMC/PVP blend loaded with ZnWO₄ or/and TPAI samples compared to undoped blends, while transmission data in the visible range reveals a small reduction with increasing TPAI concentration. As the PVA/CMC/PVP blend was doped with ZnWO₄ and TPAI amounts, the *R* values rose

irregularly. The direct and indirect E_g values of the blend diminished as it was doped with ZnWO₄ or TPAI. Compared to the undoped blend, the doped blends have the highest *n* values. The optical dielectric constants attained their highest values in the UV region. Throughout the entire wavelength range, doped blends exhibited an increase in the optical dielectric constant. Adding ZnWO₄ and TPAI samples to the host blend enhanced its σ_{opt} value in the UV range. The σ_{opt} value in the visible range changed as a function of the concentration of TPAI doping. The values of the dielectric constant and ac conductivity were affected by ZnWO₄ or TPAI doping. The M' values of the PVA/CMC/PVP blend were reduced when ZnWO₄ and TPAI samples were loaded into it. As the filler was added, the blend capacitance altered. In the visible range, the highest *n*, ϵ_r , NLO parameters were observed in the blended polymer with *x* = 0.1. The highest σ_{opt} , *k*, ϵ_i , SELF, VELF, dielectric constant parameters and ac conductivity values were detected as *x* = 0.2. The obtained properties of the formed blends make them a potential candidate for future optoelectronic and energy storage applications.

Acknowledgements This work is supported by Researchers Supporting Project number (RSP2024R72), King Saud University, Riyadh, Saudi Arabia.

Author Contributions All authors have contributed, discussed the results and approved the final manuscript.

Funding Researchers Supporting Project number (RSP2024R72), King Saud University, Riyadh, Saudi Arabia.

Data Availability No datasets were generated or analysed during the current study.

Declarations

Ethical Approval We agreed all terms and conditions for Ethics approval.

Competing Interests The authors declare no competing interests.

References

1. Z.K. Heiba, A.M. El-naggar, A.M. Kamal, M.B. Mohamed, Fabrication of soft blended- TiO₂/V/TBAI nanocomposite polymers: new trend of structural, optical and dielectric analysis for polymeric devices. *Opt. Quantum Electron.* **56**(2), 235 (2024)
2. A.M. El-naggar, Z.K. Heiba, A.M. Kamal, M.B. Mohamed, The role of cobalt amount in ZnCdS nanofiller on the optical, thermal, dielectric and structure properties of PVA/PVP/PEG blends. *Opt. Quant. Electron.* **55**(7), 609 (2023)
3. A.M. El-naggar, Z.K. Heiba, A.M. Kamal, M.B. Mohamed, Structural, linear/nonlinear optical and electrical studies on PVP/CMC blend filled with hydrogen titanate nanotubes and TMAI. *Opt. Quantum Electron.* **55**(13), 1129 (2023)
4. J.F. Rubio-Valle, M.C. Sánchez, C. Valencia, J.E. Martín-Alfonso, J.M. Franco, Electrohydrodynamic processing of PVP-Doped

- Kraft Lignin micro- and nano-structures and application of electrospun nanofiber templates to produce oleogels. *Polymers* **13**(13), 2206 (2021)
5. A.M. El Sayed, S. Saber, Structural, optical analysis, and Poole-Frenkel emission in NiO/CMC–PVP: Bio-nanocomposites for optoelectronic applications. *J. Phys. Chem. Solids* **163**, 110590 (2022)
 6. M.Z.H. Khan, M.R. Al-Mamun, P.K. Halder, M.A. Aziz, Performance improvement of modified dye-sensitized solar cells. *Renew. Sust. Energy Rev.* **71**, 602 (2017)
 7. L.P. Yee, N.K. Farhana, F.S. Omar, V. Sundararajan, S. Bashir, N.M. Saïdi, S. Ramesh, K. Ramesh, Enhancing efficiency of dye sensitized solar cells based on poly(propylene) carbonate polymer gel electrolytes incorporating double salts. *Ionics* **26**(1), 493 (2020)
 8. M.T.T. Moghadam, M. Babamoradi, R. Azimirad, Effect of hydrothermal reaction temperature on the photocatalytic properties of CdWO₄-RGO nanocomposites. *J. Nanostruct.* **9**(4), 600 (2019)
 9. J. Kim, A.I. Inamdar, Y. Jo, S. Cho, A.T.A. Ahmed, B. Hou, S.N. Cha, T.G. Kim, H. Kim, H. Im, Nanofilament array embedded tungsten oxide for highly efficient electrochromic supercapacitor electrodes. *J. Mater. Chem. A* **8**(27), 13459 (2020)
 10. A. Ali, M. Ammar, Z. Yahya, M. Waqas, M. A. Jamala, E. H. M. Salhab, A honeycomb-like ZnO/SnO₂ nanocomposite on nickel foam for high-performance asymmetric supercapacitors. *New J. Chem.* **43**(26), 10583 (2019)
 11. H. He, Z. Luo, Z.-Y. Tang, C. Yu, Controllable construction of ZnWO₄ nanostructure with enhanced performance for photosensitized Cr (VI) reduction. *Appl. Surf. Sci.* **490**, 460 (2019)
 12. M. Yin, Y. Wang, S. Liu, Synthesis of Fe₂O₃–ZnWO₄ nanocomposites and their enhanced acetone sensing performance. *J. Alloys Compd.* **831**, 154713 (2020)
 13. A. Badawi, S.S. Alharthi, The optical, electrical and mechanical performance of metal oxides incorporated PVA/rGO blend: effect of metal oxide type. *Appl. Phys. A* **128**, 328 (2022)
 14. M.A. Habeeb, W.K. Kadhim, Synthesis and tuning the structural, optical and electrical behavior of PVA-SiC–BaTiO₃ polymer nanostructures for photonics and electronics nanodevices. *J. Inorg. Organomet. Polym.* **34**, 1403 (2024)
 15. R. N. Abed, E. Yousif, A. Rahman, N. Abed, A. A. Rashad, A. Hadaway, A. H. Jawad, Optical properties of PVC composite modified during light exposure to give high absorption enhancement. *J. Non-Cryst. Solids*, **570**, 120946 (2021)
 16. Z.M. Al-Azzawi, M. Al-Baidhani, A.R.N. Abed, R.N. Abed, Influence of nano silicon carbide (SiC) embedded in Poly(Vinyl Alcohol)(PVA) lattice on the optical properties. *Silicon* **14**, 5719 (2022)
 17. A.N. Abed, R.N. Abed, Characterization effect of copper oxide and cobalt oxide nanocomposite on poly(Vinyl Chloride) doping process for solar energy applications. *Prog. Color Colorants Coat.* **15**, 235 (2022)
 18. A.S. Abouhaswa, H.M. Abomostafa, Linear and nonlinear optical properties of FeCl₃/PVA composite flexible films for optoelectronic applications. *Polym. Bull.* **81**, 3127 (2024)
 19. A.I. Alawi, E. Al-Bermany, Newly fabricated ternary PAAm-PVA-PVP blend polymer doped by SiO₂: absorption and dielectric characteristics for solar cell applications and antibacterial activity. *Silicon* **15**, 5773 (2023)
 20. S.M. Mahdi, M.A. Habeeb, Tailoring the structural and optical features of (PEO–PVA)/(SrTiO₃–CoO) polymeric nanocomposites for optical and biological applications. *Polym. Bull.* **80**, 12741 (2023)
 21. I. Oreibi, M.A. Habeeb, R.S.A. Hamza, Tailoring the structural and optical features of PVA/SiO₂-CuO polymeric nanocomposite for optical and Gamma Ray shielding applications. *Silicon* **16**, 1407 (2024)
 22. M.A. Habeeb, S.M. Mahdi, Influence of ZrC nanofiller on the structural, dielectric and optical features of the PVA–PVP blend for electronic and optical nanodevices. *Opt. Quant. Electron.* **55**, 1076 (2023)
 23. M. Kavgacı, H. Eskalen, Morphology, structure and optical properties of PVA nanocomposites reinforced with bismuth oxide nanoparticles and carbon quantum dots. *J. Mater. Sci. Mater. Electron.* **34**, 1229 (2023)
 24. H.M. Ragab, N.S. Diab, E.A.A. Elneim, N.H. El Fewaty, A.N. Al-Hakimi, M.O. Farea, Exploring the optical properties of CuCo₂O₄-doped polyethylene oxide and carboxymethylcellulose for optoelectronic application. *Opt. Quant. Electron.* **56**, 323 (2024)
 25. A. S. Abouhaswa, G. M. Turkey, T. S. Soliman, Structural, optical, and dielectric properties of PVA-CMC/Ni_{0.65}Cu_{0.35}Fe₂O₄ films for optoelectronic applications and energy storage applications. *J. Inorg. Organomet. Polym.* (2023). <https://doi.org/10.1007/s10904-023-02911-6>
 26. Z.K. Heiba, A.M. El-naggar, A.M. Kamal, M.B. Mohamed, Fabrication of soft blended- TiO₂/V/TBAI nanocomposite polymers: new trend of structural, optical and dielectric analysis for polymeric devices. *Opt. Quant. Electron.* **56**, 235 (2024)
 27. Z.K. Heiba, A.M. Kamal, A.M. El-naggar, M.B. Mohamed, M.H. Abdel-Kader, T. Alharby, Reinforcement of linear/non-linear optical and dielectric characteristics of PVC/PEG blend based on CeO₂/TBAI filler. *Inorg. Chem. Commun.* **158**, 111624 (2023)
 28. A. M. El-naggar, Z. K. Heiba, A. M. Kamal, M. B. Mohamed, Modification and development of the structural, linear/nonlinear optical and electrical characterization of PVC incorporated with iron chromium oxide and TPAI. *Opt. Quant. Electron* **55**, 982 (2023)
 29. R. Jia, Q. Wu, G. Zhang, Y. Ding, Preparation, structural and optical properties of ZnWO₄ and CdWO₄ nanofilms. *J. Mater. Sci.* **42**, 4887 (2007)
 30. R. Ricciardi, F. Auriemma, C. De Rosa, F. Laupretre, X-ray diffraction analysis of poly(vinyl alcohol) hydrogels, obtained by freezing and thawing techniques. *Macromolecules* **37**(5), 1921 (2004)
 31. Y. Golitsyna, M. Pulstb, M.H. Samiullahb, K. Busseb, J. Kresslerb, D. Reicherta, Crystallization in PEG networks: The importance of network topology and chain tilt in crystals. *Polymer* **165**(72), 72 (2019)
 32. H.E. Assender, A.H. Windle, Crystallinity in poly(vinyl alcohol). I. An X-ray diffraction study of atactic PVOH. *Polymer* **39**, 4295 (1998)
 33. A.G. El-Shamy, H.S.S. Zayied, New polyvinyl alcohol/carbon quantum dots (PVA/CQDs) nanocomposite films: Structural, optical and catalysis properties. *Synth. Met.* **259**, 116218 (2020)
 34. H. Luo, C. Yu, Z. Liu, G. Zhang, H. Geng, Y. Yi, K. Broch, Y. Hu, A. Sadhanala, L. Jiang, P. Qi, Z. Cai, H. Siringhaus, D. Zhang, Remarkable enhancement of charge carrier mobility of conjugated polymer field-effect transistors upon incorporating an ionic additive. *Sci. Adv.* **2**, e1600076 (2016)
 35. N. Alhokbany, S.M. Alshehri, J. Ahmed, Synthesis, characterization and enhanced visible light photocatalytic performance of ZnWO₄-NPs@rGO nanocomposites. *Catalysts* **11**, 153 (2021)
 36. A.O. Basheer, M.M. Hanafiah, M.A. Alsaadi, W.Z.W. Yaacob, Y. Al-Douri, Synthesis, characterization, and analysis of hybrid carbon nanotubes by chemical vapor deposition: application for aluminum removal. *Polymers* **12**(6), 1305 (2020)
 37. T.H. AlAbdulaal, W. Abdullah, I.S. Yahia, Synthesizing and exploring the structural and optical properties of PVA/ PVP/PEG polymeric sheet upon doping with nano nickel oxide (NiO) for CUT-OFF filters. *J. Mater. Res.* **27**, 8308 (2023)

38. T.H. AlAbdulaal, A. Almoadi, I.S. Yahia, H.Y. Zahran, M.S. Alqahtani, El S. Yousef, S. Alahmari, M. Jalalah, F. A. Harraz, M.S. Al-Assiri, Effects of potassium dichromate on the structural, linear/nonlinear optical properties of the fabricated PVA/PVP polymeric blends: For optoelectronics. *Mater. Sci. Eng. B* **292**, 116364 (2023)
39. R. Singh, M.S. Gaur, R.K. Tiwari, Development of polyurethane multiwall carbon nanotubes (MWCNTs) novel polymeric nanodielectric material. *J. Electrostat.* **76**, 95 (2015)
40. H. Kafashan, M. Azizieh, H.N. Vatan, Ultrasound-assisted electrodeposition of SnS: effect of ultrasound waves on the physical properties of nanostructured SnS thin films. *J. Alloy. Comp.* **686**, 962 (2016)
41. M.A. Morsi, E.M. Abdelrazek, R.M. Ramadan, I.S. Elashmawi, A. Rajeh, Structural, optical, mechanical, and dielectric properties studies of carboxymethyl cellulose/polyacrylamide/lithium titanate nanocomposites films as an application in energy storage devices. *Polym. Test.* **114**, 107705 (2022)
42. H.E. Ali, I. Morad, H. Algarni, M. M. El-Desoky, Y. Khairy, H.Y. Zahran, I.S. Yahia, Structure analysis and nonlinear/linear optical properties of PVAOH/Si composites for low-cost optical technologies and limiting absorption. *J. Mater. Sci. Mater. Electron.* **32**, 4466 (2021)
43. M.B. Mohamed, M.H. Abdel-Kader, Effect of annealed ZnS nanoparticles on the structural and optical properties of PVA polymer nanocomposite. *Mater. Chem. Phys.* **241**, 122285 (2020)
44. S.B. Aziz, H.M. Ahmed, A.M. Hussein, A.B. Fathulla, R.M. Wsw, R.T. Hussein, Tuning the absorption of ultraviolet spectra and optical parameters of aluminum doped PVA based solid polymer composites. *J. Mater. Sci. Mater. Electron.* **26**, 8022 (2015)
45. S.B. Aziz, Modifying Poly(Vinyl Alcohol) (PVA) from insulator to small-bandgap polymer: a novel approach for organic solar cells and optoelectronic devices. *J. Electron. Mater.* **45**, 736 (2016)
46. G.R. Suma, N.K. Subramani, K.N. Shilpa, S. Sachhidananda, S.V. Satyanarayana, Effect of $Ce_{0.5}Zr_{0.5}O_2$ nano fillers on structural and optical behaviors of poly(vinyl alcohol), *J. Mater. Sci. Mater. Electron.* **28**(14), 10707 (2017)
47. M.S. Ismail, A.A. Elamin, F. Abdel-Wahab, Y.H. Elbasha, M.M. Mahasen, Improving the refractive index by engineering PbS/PVA nano polymer composite for optoelectronic applications. *Opt. Mater.* **131**, 112639 (2022)
48. Q.M.A. Hassan, H. Bakr, C.A. Emshary, H.A. Sultan, Studying the surface morphology, optical and nonlinear optical properties of epoxy resin doped nickel nitrate film. *Optik* **213**, 164771 (2020)
49. G. Raja, S. Gopinath, R. Azhagu, A.K. Shukla, M.S. Alhoshan, K. Sivakumar, *J. Phys. E* **158**, 69 (2016)
50. S. Elashmawi, A.M. Abdelghany, N.A. Hakeem, Quantum confinement effect of CdS nanoparticles dispersed within PVP/PVA nanocomposites. *J. Mater. Sci. Mater. Electron.* **24**, 2956 (2013)
51. F.N.G. Imam, M.B. Mohamed, Flower-like morphology of blue and greenish-gray $ZnCoAl_2-xO_4$ nanopigments. *J. Mol. Struct.* **1105**, 80 (2016)
52. A. Saeed, M.S. Al-Buriahi, M.A.N. Razvi, N. Salah, F.E. Al-Hazmi, Electrical and dielectric properties of meridional and facial Alq3 nanorods powders. *J. Mater. Sci. Mater. Electron.* **32**(2), 2075 (2021)
53. G. Kandhol, H. Wadhwa, S. Chand, S. Mahendia, S. Kumar, Study of dielectric relaxation behavior of composites of Poly (vinyl alcohol) (PVA) and Reduced graphene oxide (RGO). *Vacuum* **160**, 384 (2019)
54. A.Y. Yassin, Dielectric spectroscopy characterization of relaxation in composite based on (PVA–PVP) blend for nickel– cadmium batteries. *J. Mater. Sci. Mater. Electron.* **31**, 19447 (2020)
55. A.Y. Yassin, A. Raouf Mohamed, A.M. Abdelghany, E.M. Abdelrazek, Enhancement of dielectric properties and AC electrical conductivity of nanocomposite using poly (vinyl chloride-co-vinyl acetate-co-2-hydroxypropyl acrylate) filled with graphene oxide. *J. Mater. Sci. Mater. Electron.* **29**, 15931 (2018)
56. S.A. Mohamed, A.A. Al-Ghamdi, G.D. Sharma, M.K. El Mansy, Effect of ethylene carbonate as a plasticizer on CuI/PVA nanocomposite: structure, optical and electrical properties. *J. Adv. Res.* **5**, 79 (2014)
57. M.M. Abdelhamied, A.M. Abdelreheem, A. Atta, Plastics, influence of ion beam and silver nanoparticles on dielectric properties of flexible PVA/PANI polymer composite films. *Rubber Compos.* **51**(1), 1 (2022)
58. S. Yu, P. Hing, X. Hu, Dielectric properties of polystyrene– aluminum-nitride composites. *J. Appl. Phys.* **88**(1), 398 (2000)
59. F.S. Howell, R.A. Bose, P.B. Macedo, C.T. Moynihan, Electrical relaxation in a glass-forming molten salt. *J. Phys. Chem.* **78**(6), 639 (1974)
60. J. Naik, R.F. Bhajantri, S.G. Rathod, T. Sheela, V. Ravindrachary, Synthesis and characterization of multifunctional ZnBr 2/PVA polymer dielectrics. *J. Adv. Dielectr.* **06**(04), 1650028 (2016)
61. M.M. Damoom, A. Saeed, E.M. Alshammari, A.M. Alhawsawi, A.Y. Yassin, J.A. Mohammed Abdulwahed, A.A. Al-Muntaser. The role of TiO₂ nanoparticles in enhancing the structural, optical, and electrical properties of PVA/PVP/CMC ternary polymer blend: nanocomposites for capacitive energy storage. *J. Sol-Gel Sci. Technol.* **108**, 742 (2023)

Publisher's Note Springer Nature remains neutral with regard to jurisdictional claims in published maps and institutional affiliations.

Springer Nature or its licensor (e.g. a society or other partner) holds exclusive rights to this article under a publishing agreement with the author(s) or other rightsholder(s); author self-archiving of the accepted manuscript version of this article is solely governed by the terms of such publishing agreement and applicable law.